

Theoretical predictions of structural phase transitions in Cr, Mo, and W

P. Söderlind, R. Ahuja, O. Eriksson, and B. Johansson

Condensed Matter Theory Group, Department of Physics, University of Uppsala, Box 530, Uppsala, Sweden

J. M. Wills

Center for Materials Science and Theoretical Division, Los Alamos National Laboratory, Los Alamos, New Mexico 87545

(Received 30 November 1993)

Theoretical predictions, based on local-density calculations, of pressure-induced structural phase transitions in Cr, Mo, and W are reported. Phase changes at high compressions are found for all three metals. As a function of compression the structural sequence $bcc \rightarrow hcp \rightarrow fcc \rightarrow bcc$ is found for Cr and Mo. For W, the structural sequence $bcc \rightarrow hcp \rightarrow fcc$ was found. Calculations for W were performed down to about 30% of the ambient volume, whereas Cr and Mo were studied at compressions down to about 10% of the experimental volume. The structural sequence $bcc \rightarrow hcp \rightarrow fcc$ for Cr, Mo, and W can be understood from band-filling arguments, while the fact that the bcc crystal structure, found at ambient conditions, becomes stable at extreme compression (at volumes typically 10% of the experimental volume) for Cr and Mo is explained by the gradually increased p - d overlap and hybridization in these elements under compression.

I. INTRODUCTION

The crystal structure sequence at ambient pressure for the d transition elements has been accurately accounted for by means of *ab initio* local-density calculations¹ almost a decade ago. Today, static pressures up to several Mbar can be attained in the diamond anvil cell, which have led to new experimental^{2,3} achievements. As a consequence of the new experimental data there is also an increased theoretical³⁻⁶ interest in the structural phase transitions in the d transition elements under very high compressions. In the present investigation we have concentrated our theoretical efforts to the elements of the VIB group, namely Cr, Mo, and W.

Cr has been studied extensively, mostly with emphasis on its interesting magnetic structure. There are, however, a few reports on the behavior of Cr at high pressures. Mattheiss *et al.*⁶ found from linearized augmented plane wave (LAPW) calculations that the structural energy difference between Cr (bcc) and Cr (fcc) was very large at ambient pressure and questioned the experimentally reported fcc phase of Cr.⁷ Furthermore, these authors⁶ also found an even larger structural energy difference between the fcc and bcc crystal structures for Mo and W. Since in these calculations a frozen core approximation was used they were unable to study accurately the total energies at large compression. This was instead done by Singh⁴ who investigated Cr together with Mo and W theoretically by means of a pair potential method at high pressures. Moriarty⁵ also studied these three elements theoretically at ultrahigh pressures, and for Cr he found a phase transition $bcc \rightarrow hcp$ at a volume about half of the experimental equilibrium volume (V_{expt}), whereas Singh⁴ has reported first a $bcc \rightarrow hcp$ and then an $hcp \rightarrow fcc$ transition at a volume of about $0.6V_{\text{expt}}$.

Cr is experimentally known to be an itinerant magnet with a rather complex magnetic structure. Also theoretically the antiferromagnetic phase has been found to be favored.⁸ The calculated magnetic moment is however suppressed considerably already at a pressure of about 200 kbar.⁹ In our treatment of Cr under compression we only consider the paramagnetic state. This is justified since the expected phase transition occurs at high compressions where the magnetism has disappeared. Apart from the presence of magnetism the properties of Cr are very similar to the $4d$ (Mo) and the $5d$ (W) counterparts. These latter two elements have received a lot of theoretical³⁻⁶ and experimental^{2,3,10} attention recently. Mo is an interesting element in the present context since it is used in the calibration of the ruby fluorescence technique in connection with ultrahigh-pressure static experiments. Furthermore, it is of interest to note that these isoelectronic elements, which at ambient pressure all are very stable in the bcc crystal structure and at the same time are even locally unstable in the fcc crystal structure,¹¹ are predicted to transform to the fcc state at large compression.¹²

The rapid development of high-pressure techniques has led to a renewed interest in the phase transitions of the transition metals. Experimentally it has earlier been difficult to perform measurements in the multimegabar range, which often is needed to drive phase transitions in the transition metals. However this can now be done and a solid-solid phase transition of Mo was indeed found³ in a shock compression experiment at a pressure of 2.1 Mbar and a temperature of 4100 K. This transition was seen as a discontinuity in the acoustic sound velocity. Together with theoretical calculations³ this transition was concluded to be a $bcc \rightarrow hcp$ transition. The calculations³ were done within the atomic sphere approximation, where the charge density and one-electron potential are assumed to be spherical. Furthermore Andersen's force theorem¹³ was used and this gave a bcc

→ hcp transition pressure of 3.2 Mbar at $V = 0.62V_{\text{expt}}$. Recently, a study of Mo under static compression, using a diamond anvil cell in connection with energy dispersive x-ray diffraction using a synchrotron source was published.² The ambient bcc phase was in this investigation found to be stable over a pressure range up to 4.2 Mbar with a corresponding volume compression of $V/V_{\text{expt}} = 0.58$, in disagreement with the result of Hixon *et al.*³ However, this result is consistent with a theoretical calculation by Sikka *et al.*¹⁴ who did not obtain a bcc → hcp transition at compression down to $0.57V_{\text{expt}}$. Moriarty⁵ on the other hand has lately reported a bcc → hcp transition in Mo at $V = 0.58V_{\text{expt}}$ and a calculated transition pressure of 4.2 Mbar in disagreement with the static diamond anvil cell experiment.²

The last of the considered elements, W, has been studied by many authors who primarily use this metal as a test object for their computational techniques.^{6,15,16} But as mentioned above, both Singh⁴ and Moriarty⁵ have done calculations on W which are relevant for this work, and below we will compare our calculated data with theirs.

The remaining part of the paper is organized as follows. In Sec. II we describe briefly the computational technique which has been used in order to calculate total energies with a mRy accuracy. Here we also account for the treatment of the so-called “core,” “pseudocore,” and “valence” electrons. In Sec. III the structural energies, which are the primary results of this work, are reported. Finally, in Sec. IV, we present our conclusions.

II. DETAILS OF THE CALCULATIONS

The present computational method¹⁷ is based upon the linear muffin-tin orbital (LMTO) technique¹⁸ in the implementation of the Kohn-Sham local-density theory,¹⁹ with the Hedin-Lundqvist²⁰ exchange-correlation functional. The method involves a consideration of all the electrons and is fully relativistic in the sense that the spin-orbit coupling is introduced in the variational step.¹⁸ The electron charge density and the effective potential are not restricted to be spherical, something which is accomplished by dividing the unit cell into a spherical muffin tin and a so-called interstitial region. In the interstitial region the potential is represented by a Fourier expansion, whereas inside the muffin tins the expansion consists of spherical harmonic functions together with a radial function. It is essential to be able to handle the electrons which are at the borderline between lying very deep in energy, and being part of a chemically inert ionic core, and the electrons which are part of the valence band. These borderline electron states (pseudocore) become increasingly important when a given element is exposed to large compressions. Therefore we were forced to use a larger set of augmented LMTO's than what is usually done in order to represent those “pseudocore” electron states adequately. For Cr the basis set therefore consists of $3s$, $3p$, $4s$, $4p$, and $3d$ partial waves whereas for Mo the $4s$, $4p$, $5s$, $5p$, and $4d$ partial waves are utilized. For W the corresponding $5s$, $5p$, $6s$, $6p$, and $5d$ partial

waves are included in the basis set. Two sets of energy parameters are used, one appropriate for the lower lying s and p states of the “pseudocore” and another for the valence band states. The convergence of the electronic structure calculations in \mathbf{k} space is increasingly important for a solid at very large volume compressions. The Brillouin zone (BZ) becomes larger, and more \mathbf{k} points are generally needed. The bcc and fcc crystal structures were treated as bct with $c/a = 1.0$ and $c/a = \sqrt{2}$, respectively, and for these structures 4096 \mathbf{k} points in the full BZ were used. For the hexagonal structure we found that 3072 \mathbf{k} points in the full BZ were sufficient to use.

We end this section with a comparison of the present computational method and some of the previous calculations. First of all the present theory does not rely on approximations concerning the shape of the potential. This is in contrast to the calculations presented earlier^{3,5,14} which relied on the atomic sphere approximation (ASA). Also, the present calculations are relativistic and incorporate for instance the mass-velocity, Darwin shift, and spin-orbit interaction. The latter term was neglected in the previous treatments.^{3,5,14} Another advantage with our calculations is that the basis set consists of functions that represent states of electrons that usually are defined as being part of a frozen core.^{3,14} This was done in a single fully hybridizing panel. Finally, we used a so-called double basis where two different Hankel (or Neuman) functions with different kinetic energy were matched onto two different basis functions inside the muffin-tin sphere. The resulting basis set has a better variational freedom than the “standard” LMTO-ASA basis.^{3,5,14}

III. STRUCTURAL ENERGIES

In the present investigation of Cr we have studied three crystal structure phases; bcc, fcc, and hcp [with an ideal $c/a = (\frac{8}{3})^{1/2}$]. This has been done over a wide pressure range. In Fig. 1 we show the total energy of bcc Cr as a function of volume and in the inset the energy difference between the bcc, fcc, and hcp phases in Cr. The energies are normalized with respect to the fcc phase which defines the zero energy of the plot. The transition volumes and pressures, to be discussed below, are collected in Table I, together with earlier computed and measured results. Down to about $0.4V_{\text{expt}}$ the bcc phase of Cr is lowest in energy in good agreement with the theoretical results obtained by Singh.⁴ Our calculated energy difference is, however, considerably larger for all volumes than the energy difference found by Singh,⁴ and our energies at ambient conditions compare better with other reported results.^{1,6} The hcp phase is energetically very close to the fcc phase over most of the considered volume range, which is most reasonable since the two structures have the same first- and second-nearest-neighbor distance. At volumes lower than $0.4V_{\text{expt}}$ the hcp phase of Cr becomes more stable than the fcc and bcc phases. Then at a slightly larger compression the fcc phase becomes the most favorable structure. The fact that the fcc structure becomes stable at high pressures was previously

TABLE I. Summary of current theoretical and experimental results for the crystal structures of Cr, Mo, and W at ultrahigh pressure. The pressures are in Mbar. V_{expt} for Cr, Mo, and W is 12.00 \AA^3 , 15.49 \AA^3 , and 15.85 \AA^3 , respectively. "Shock data" and "static data" represent experimental observations under shock and static compressions, respectively.

Element	Description	bcc \rightarrow hcp		hcp \rightarrow fcc		fcc \rightarrow bcc	
		P	V/V_{expt}	P	V/V_{expt}	P	V/V_{expt}
Cr	This work	12.5	0.39	17.2	0.35	494	0.107
	Moriarty ^a	7.0	0.47	—	—	—	—
	Singh ^b	—	~ 0.4	—	~ 0.4	—	—
Mo	This work	5.2	0.55	7.4	0.50	340	0.128
	Moriarty ^a	4.2	0.58	6.2	0.515	—	—
	Hixon ^c	3.2	0.62	4.7	0.56	—	—
	Singh ^b	—	~ 0.6	—	~ 0.6	—	—
	Sikka ^d	>4.9	<0.57	—	—	—	—
	Shock data ^e	2.1	—	—	—	—	—
	Static data ^e	>4.2	<0.58	—	—	—	—
W	This work	9.2	0.49	14.4	0.43	—	—
	Moriarty ^a	12.5	0.44	14.4	0.42	—	—
	Singh ^b	—	~ 0.6	—	~ 0.6	—	—
	Shock data ^a	4.3	—	—	—	—	—
	Static data ^f	>3.78	<0.62	—	—	—	—

^aMoriarty (Ref. 5).

^bSingh (Ref. 4).

^cHixon *et al.* (Ref. 3).

^dSikka *et al.* (Ref. 14).

^eVohra *et al.* (Ref. 2).

^fRuoff *et al.* (Ref. 26).

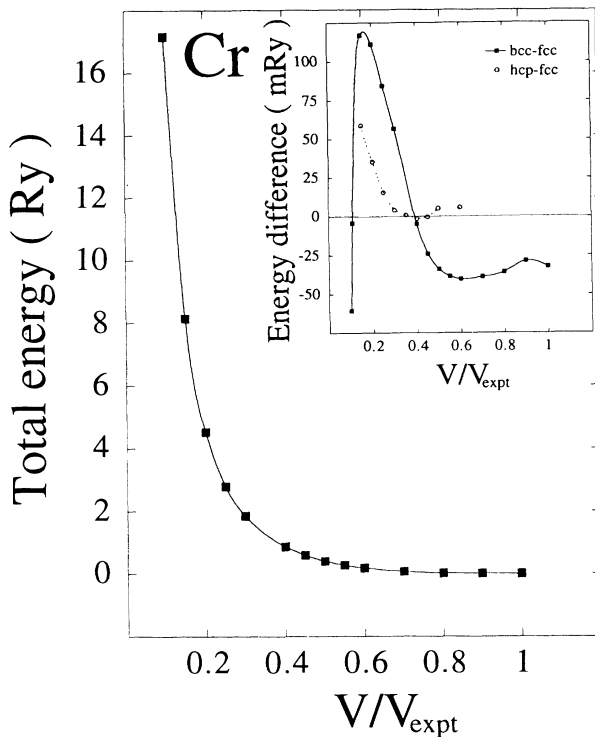


FIG. 1. Calculated total energies for Cr normalized so that the energy at V_{expt} is equal to zero. The squares denote the bcc crystal structure energies and the line is a fit that serves as a guide for the eye. The inset displays the structural energy differences with the fcc crystal structure defining the zero level. The filled squares and open circles denote the bcc and hcp energies, respectively.

found by Singh,⁴ but in our calculation this happens at a slightly larger compression. For even higher compressions, the energy of the fcc phase initially increases, but at $\sim 10\%$ of V_{expt} the relative energy of the bcc phase drops dramatically, as can be seen in Fig. 1. We are not aware of any previous results predicting this transition in Cr. For a system at such a high density one might expect the electrostatic Madelung energy to become very important. However, we show in Fig. 2 that

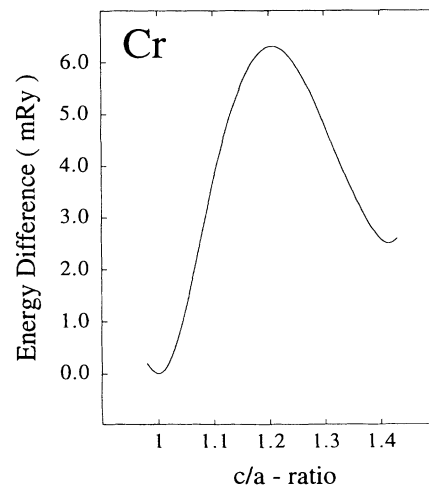


FIG. 2. Estimate of the Madelung energy in Cr at about 10% of the experimental volume for the bct crystal structure as a function of the c/a ratio. The Madelung energy for the bcc crystal structure ($c/a = 1.0$) is used as a reference energy.

this is not the case. Here we show an estimate of the Madelung energy as a function of the c/a ratio in the bct crystal structure ($c/a = 1$ for bcc and $c/a = \sqrt{2}$ for fcc). In this figure the Madelung energy is estimated as²¹ $U = -\alpha Q^2/S$ where α is the Madelung (or Ewald) constant and S is the Wigner-Seitz radius. The effective nuclear charge Q is the unit cell volume times the average interstitial electron density. The small energy barrier between the bcc and fcc structures, of about 6 mRy in Fig. 2, reflects the fact that the Madelung contribution is of almost negligible importance for Cr at this compression (the variation of the total energy at this compression is of the order of 100 mRy, see Fig. 1). Instead the largest contribution to the total energy comes from the band energy term (E_b). At this low volume the d density of states (DOS) has become extremely broad and the typical features found for the bcc and the fcc crystal structure in the DOS at normal or moderate pressures are no longer visible. In Fig. 3 we show that the total DOS for the bcc, fcc, and bct ($c/a = 1.2$) structures

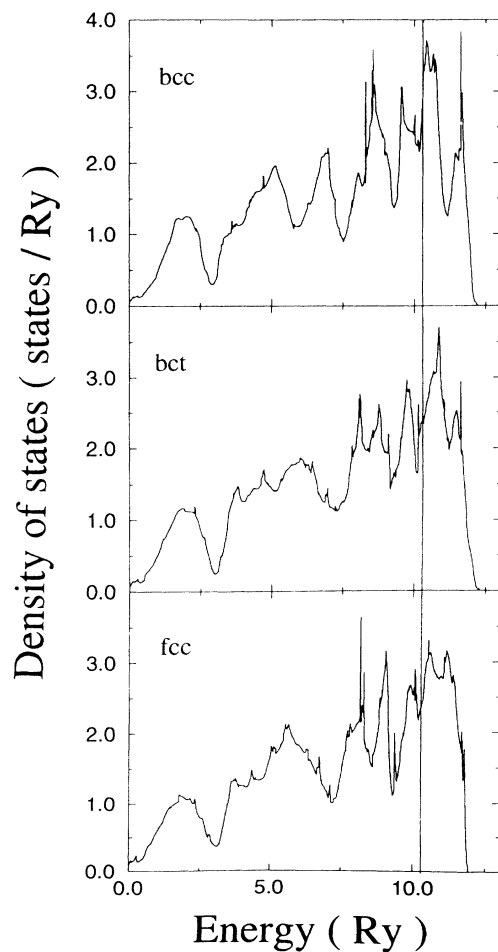


FIG. 3. Total density of states (states/Ry) for bcc, bct, and fcc Cr at $\sim 10\%$ of the experimental volume. The bcc and fcc DOS of Cr are plotted in the upper and lower panels, respectively. In the middle panel Cr has a bct structure with $c/a = 1.2$. Energies are in Rydbergs and E_F is marked by a vertical line.

are very similar. Furthermore it is obvious that these DOS are very broad and as a first approximation almost free-electron-like with a dependence of the DOS which is roughly proportional to \sqrt{E} . This is further illustrated in Fig. 4 where we compare the bcc DOS with the DOS from the free-electron model, $D_{\text{FEM}}(E) = \frac{V}{2\pi^2} \sqrt{E}$ [using atomic units where $\hbar^2/(2m) = 1$]. In Fig. 4 the volume of Cr is about 10% of V_{expt} . The free-electron model gives a higher Fermi energy (E_F) (13.1 Ry as compared to 10.3 Ry from the calculations) so that the FEM DOS is lying somewhat lower than our calculated DOS. Apart from the detailed structure of the DOS obtained from the full calculation, the free-electron DOS and the theoretical DOS display approximately a similar behavior. The fact that the calculated DOS for the three different crystal structures are very similar (they are all similar to the free electron DOS) would imply that the differences in E_b between Cr in the different crystal structures are small. This is, however, balanced by the fact that the bands are extremely broad and that E_b roughly scales with the width of the band. Hence, due to the change of the d occupation as well as due to a modification of the shape of the d DOS, paramagnetic Cr is predicted to display a most extraordinary phase diagram at zero temperature, with a crystallographic structure sequence bcc \rightarrow hcp \rightarrow fcc \rightarrow bcc. It is of particular interest to note the reappearance of the bcc phase at highly compressed volumes. There are however no experimental data as regards crystallographic phase transitions in Cr available that we are aware of.

In Fig. 5 we show the calculated structural energies of the $4d$ counterpart of Cr, namely Mo. This metal is a member of the same group (VIB) of elements in the Periodic Table as Cr, and shows very much the same crystal structure behavior as a function of volume as Cr. At V_{expt} Mo (as well as Cr and W) is very stable in the

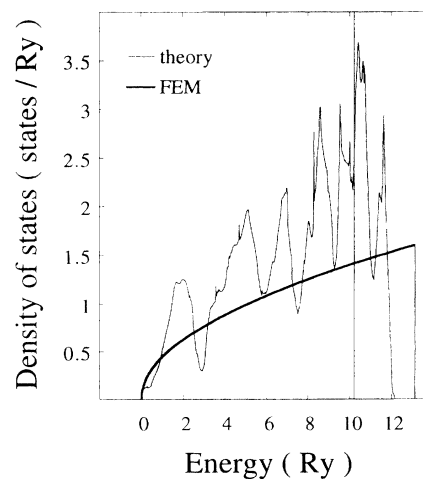


FIG. 4. Total theoretical (theory) DOS for Cr in the bcc structure together with a free-electron model (FEM) DOS (see text). The units of the DOS are in states/Ry and the energy units are in Rydbergs. The Fermi level for the theoretical DOS is at 10.3 Ry and for the model DOS at 13.1 Ry.

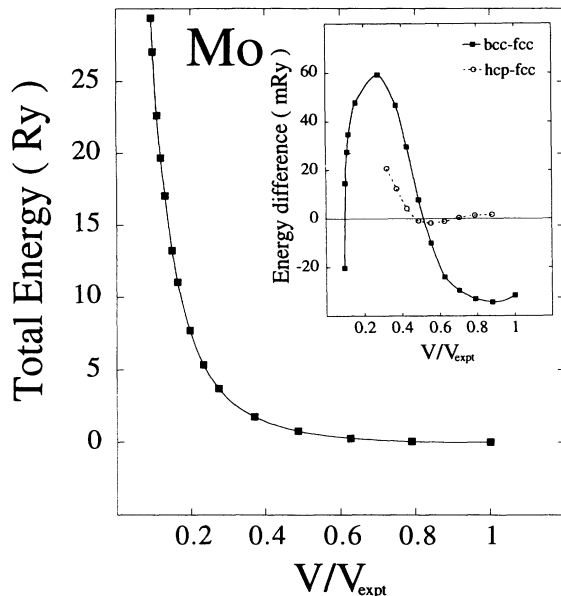


FIG. 5. Calculated total energies for Mo normalized so that the energy at V_{expt} is equal to zero. The squares denote the bcc crystal structure energies and the line is a fit that serves as a guide for the eye. The inset displays the structural energy differences with the fcc crystal structure defining the zero level. The filled squares and open circles denote the bcc and hcp energies, respectively.

bcc phase due to the fact that E_F is lying in the middle between the two characteristic peaks (E_g and T_{2g}) of the bcc d DOS (not shown). In fact it is known from theoretical calculations that Mo (and W) do not even have a metastable fcc phase at ambient pressure, i.e., the fcc crystal structure is transforming spontaneously to the bcc crystal structure.¹¹ The energy difference between the bcc and the fcc phases of Mo is approximately the same as found for Cr at normal pressure and the general behavior is similar with a parabolic-like increase as a function of compression. However, at a volume of about $0.55V_{\text{expt}}$, the hcp structure (with ideal c/a ratio) becomes stable and thereafter the fcc crystal structure is favored as can be seen from Fig. 5 and Table I. The fcc phase then becomes stable whereas in the volume interval $0.5-0.3V_{\text{expt}}$ both the bcc as well as the hcp structure show an increase of the energy in comparison to the fcc structure. As already mentioned, the fcc and the hcp crystal structures are very similar, and so are their corresponding DOS. However, even small differences in the DOS can result in a relatively large band energy difference at high volume reductions due to the broadening of the bands under compression. The present results for Mo are essentially a confirmation of the results reported by Hixon *et al.*³ and Moriarty⁵ even though their transition volume (bcc \rightarrow hcp) was calculated to be at $0.62V_{\text{expt}}$ and $0.58V_{\text{expt}}$, respectively, in comparison to our calculated transition volume of $0.55V_{\text{expt}}$ (see Table I). Our results agree better with the calculation of Sikka *et al.*¹⁴ who did not find a bcc \rightarrow hcp transition down

to $0.57V_{\text{expt}}$ at a pressure of 4.9 Mbar. In earlier work^{3,5} the crystallographic phase transition from bcc \rightarrow hcp in Mo is explained to be due to an increased d occupation caused by a pressure-induced $sp \rightarrow d$ transfer. This description, where the bcc \rightarrow hcp transition is regarded as due to an increase of the d valence occupancy, is analogous to the behavior of the crystallographic structure sequence hcp \rightarrow bcc \rightarrow hcp \rightarrow fcc in the $4d$ and $5d$ transition metals at ambient conditions. From the Periodic Table we know that Tc, which has about one more d electron than Mo, is hcp at zero pressure. Therefore there should be a critical d occupation, in for instance Mo under compression or in $\text{Mo}_{1-x}\text{Tc}_x$ alloys, for which the energy of the bcc and hcp phases coincide. In an approximative picture where the shape of the d DOS of Mo is considered as rigid, the increase of the d occupation can be accomplished by either compressing the metal or by alloying with Tc. Hence, by studying compressed Mo and the alloy $\text{Mo}_{1-x}\text{Tc}_x$, the argument that the d band filling (i.e., the band energy of the d DOS) determines the crystal structure can be tested. In order to simplify the picture we have chosen to study the fcc rather than the hcp crystal structure for Mo (the fcc and hcp structures are very close in energy). The advantage of studying the fcc structure in the present context is that the fcc structure as well as the bcc structure can be viewed as a special case of the body centered tetragonal (bct) structure. Thus, in Fig. 6 we show the total energy for compressed Mo as well as for a $\text{Mo}_{1-x}\text{Tc}_x$ ($x = 0.6$) alloy in the bct structure as a function of the c/a ratio. This is the so-called Bain transformation path,²² which brings the crystal from the bcc ($c/a = 1.0$) to the fcc ($c/a = \sqrt{2}$) structure. For Mo the volume is compressed to $V=0.5V_{\text{expt}}$ whereas $\text{Mo}_{0.4}\text{Tc}_{0.6}$ is calculated in the virtual crystal approximation²³ (VCA) at ambient pressure. This approximation is in accordance with our assumption of a rigid d band shape. Furthermore, the VCA has recently been used successfully in calculations of the elastic constants for d transition metal alloys.¹¹

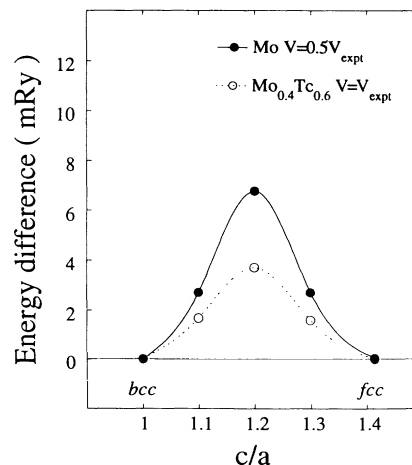


FIG. 6. The Bain path, i.e., the energy as a function of c/a in the bct crystal structure, for the $\text{Mo}_{1-x}\text{Tc}_x$ alloy (see text) and compressed Mo.

From Fig. 6 we conclude that these two systems behave very similar under a tetragonal transformation, and that the increase of the energy when lowering the crystal symmetry (i.e., $1.0 < c/a < \sqrt{2}$) is small. Thus, for Mo compressed down to $0.5V_{\text{expt}}$ the first moment energy (or band energy) term to a large extent dictates the crystal structure and we conclude that the Madelung energy, which is a Coulomb energy that depends on the crystal structure and the charge density,¹ is less important. This conclusion is in agreement with earlier explanations of phase transitions in group VIB elements.^{3,5} At even higher compression, Mo shows the same behavior as Cr, i.e., the bcc structure becomes stable at the very lowest volumes. The critical volume for this transition, both in Cr and Mo, is roughly 10% of V_{expt} . The pressure is calculated to be about 350 Mbar at this compression for Mo (see Table I).

For W we obtain, in agreement with Singh⁴ and Moriarty,⁵ a bcc \rightarrow hcp transition (Table I), but in our calculations this transition occurs at a transition volume $\sim 0.5V_{\text{expt}}$, while Singh⁴ and Moriarty⁵ report a transition volume of $\sim 60\%$ and 44% , respectively. Moriarty calculated the transition pressure of the bcc \rightarrow hcp transition for W to be 12.5 Mbar and he also found a subsequent transition (hcp \rightarrow fcc) at a pressure of 14.4 Mbar. We display our results in Fig. 7 where for W, similarly to Mo and Cr, the hcp phase becomes stable at a pressure of 9.2 Mbar ($V = 0.49V_{\text{expt}}$). The fcc phase is only marginally higher than the hcp structure at this volume and for increasing compression the fcc phase follows

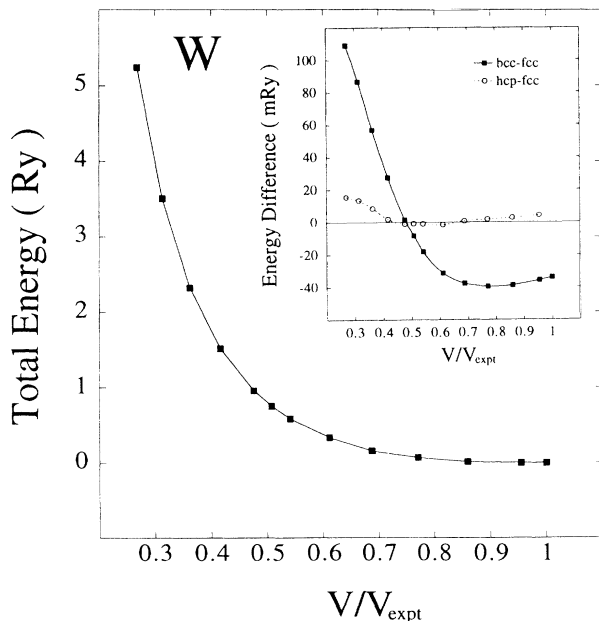


FIG. 7. Calculated total energies for W normalized so that the energy at V_{expt} is equal to zero. The squares denote the bcc crystal structure energies and the line is a fit that serves as a guide for the eye. The inset displays the structural energy differences with the fcc crystal structure defining the zero level. The filled squares and open circles denote the bcc and hcp energies, respectively.

the same behavior as found for Cr and Mo and becomes more stable. For W our results agree well with the results of Moriarty,⁵ the hcp \rightarrow fcc transition occurs at 14.4 Mbar and at a volume $V \sim 0.43V_{\text{expt}}$. In spite of the fact that Mo and W belong to the same group of elements, and therefore show a strong similarity of the electronic structure, there are some differences. W is a rather heavy element and the relativistic effects on the electronic structure are therefore non-negligible. Furthermore the $4f$ states can hybridize with the $5s$ and $5d$ bands at extreme compressions, leading to a behavior of W that differs slightly from Mo.

IV. CONCLUSIONS

The elements Cr, Mo, and W show pronounced similarities in their crystallographic behavior. All three elements are bcc at ambient conditions and under high pressure transform to hcp and fcc. The transition bcc \rightarrow hcp occurs at a volume compression of approximately 30%–50% of V_{expt} , and by comparing the Bain path for Mo at this compression with a $\text{Mo}_{1-x}\text{Tc}_x$ ($x = 0.6$) alloy with a corresponding d occupation, we draw the conclusion that it is the band filling that dictates the crystal structure, and not the Madelung contribution to the total energy. Down to this compression the DOS is still approximately rigid.

For Cr and Mo we have performed calculations at extraordinary high compressions, at about 10% of the experimental volume. We conclude that the reappearance of the bcc structure at these volumes is associated with a breakdown of the rigid band picture. The strongly modified DOS becomes free-electron-like and very broad at these compressions. Surprisingly, the electrostatic energy for the crystal structure at this compression is not of any decisive importance. At high compression the broadened bands, together with the tendency for high angular

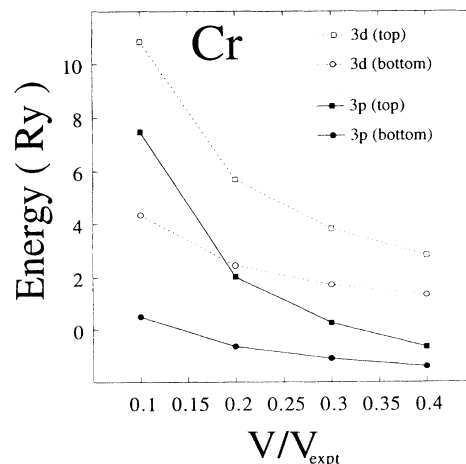


FIG. 8. Top and bottom of the Cr $3p$ and $3d$ bands, respectively. The d band is denoted with open symbols and dotted lines whereas the p band is denoted with filled symbols and a full line. The energy is in Rydbergs.

momentum bands to drop in energy relative to those of lower angular momentum, will lead to an increased p - d overlap and hybridization. This is demonstrated in Fig. 8 where the top and bottom of the $3p$ and $3d$ bands in Cr are shown. The top of the $3p$, and the bottom of the $3d$ bands coincide at a volume of about $0.18V_{\text{expt}}$ which is at a volume somewhat larger than the calculated critical volume for the fcc \rightarrow bcc transition in Cr. We have used the Wigner-Seitz rule to estimate the top and bottom of the bands in Fig. 8.

According to the arguments of McMahan²⁴ the “pseudocore” valence band hybridization stabilizes the bcc structure in Cs. For highly compressed Cr, Mo, and W this hybridization is also important and to substantiate this statement we have performed model calculations us-

ing canonical p and d bands which are allowed to hybridize. These calculations (to be published in more detail elsewhere²⁵) show, in agreement with McMahan,²⁴ that the p - d hybridization stabilizes the bcc structure in Cr, Mo, and W at very high pressures. As a matter of fact these calculations predict that most materials should adopt the bcc structure at very high pressures.

ACKNOWLEDGMENTS

We wish to acknowledge A. K. McMahan for valuable comments, and J. Trygg and T. Gasche for encouraging discussions.

-
- ¹ H. L. Skriver, Phys. Rev. B **31**, 1909 (1985).
² Y. K. Vohra and L. A. Ruoff (unpublished).
³ R. S. Hixon, D. A. Boness, J. W. Shaner, and J. A. Moriarty, Phys. Rev. Lett. **62**, 637 (1989).
⁴ N. Singh, Phys. Rev. B **46**, 46 (1992).
⁵ J. A. Moriarty, Phys. Rev. B **45**, 2004 (1992).
⁶ L. F. Mattheiss and D. R. Hamann, Phys. Rev. B **33**, 823 (1986).
⁷ R. E. Thomas and G. A. Haas, J. Appl. Phys. **43**, 4900 (1972).
⁸ J. Kübler, J. Magn. Magn. Mater. **20**, 262 (1980).
⁹ H. L. Skriver, J. Phys. F **11**, 97 (1981).
¹⁰ B. K. Godwal and Raymond Jeanloz, Phys. Rev. B **41**, 7440 (1990).
¹¹ P. Söderlind, O. Eriksson, J. M. Wills, and A. M. Boring, Phys. Rev. B **48**, 5844 (1993).
¹² Y. Ohta and M. Shimizu, J. Phys. F **15**, 927 (1985).
¹³ A. R. Mackintosh and O. K. Andersen, in *Electrons at the Fermi Surface*, edited by M. Springford (Cambridge University Press, Cambridge, 1980).
¹⁴ S. K. Sikka, B. K. Godwal, and R. S. Rao, *High Pressure Research* (Gordon and Breach, United Kingdom, 1992), Vol. 10, 707.
¹⁵ H. J. Jan, Phys. Rev. B **30**, 561 (1984).
¹⁶ C. T. Chan, David Vanderbilt, and Steven G. Louie, Phys. Rev. B **33**, 7941 (1986).
¹⁷ J. M. Wills (unpublished); J. M. Wills and B. R. Cooper, Phys. Rev. B **36**, 3809 (1987).
¹⁸ O. K. Andersen, Phys. Rev. B **12**, 3060 (1975).
¹⁹ W. Kohn and L. J. Sham, Phys. Rev. **140**, A1133 (1965).
²⁰ U. von Barth and L. Hedin, J. Phys. C **5**, 1629 (1972).
²¹ E. Esposito, A. E. Carlsson, David D. Ling, H. Ehrenreich, and C. D. Gelatt, Jr., Philos. Mag. **41**, 251 (1980).
²² I. C. Bain, Trans. AIME **70**, 25 (1924).
²³ This means that the alloy consists of “average” atoms with a concentration weighted atomic number.
²⁴ A. K. McMahan, Phys. Rev. B **29**, 5982 (1984).
²⁵ R. Ahuja, P. Söderlind, J. Trygg, J. Melsen, J. M. Wills, B. Johansson, and O. Eriksson (unpublished).
²⁶ A. L. Ruoff, H. Xia, H. Luo, and Y. K. Vohra, Rev. Sci. Instrum. **61**, 3830 (1990).